HHS Public Access

Author manuscript

Pain. Author manuscript; available in PMC 2024 January 01.

Published in final edited form as:

Pain. 2023 January 01; 164(1): 119–131. doi:10.1097/j.pain.0000000000002673.

E74-like factor 1 contributes to nerve trauma-induced nociceptive hypersensitivity via transcriptionally activating matrix metalloprotein-9 in dorsal root ganglion neurons

Luyao Zhang[a,*], **Xiang Li**[a,*], **Xiaozhou Feng**[a,*], **Tolga Berkman**[a], **Ruining Ma**[a], **Shibin Du**[a], **Shaogen Wu**[a], **Congcong Huang**[a], **Akwasi Amponsah**[a], **Alex Bekker**[a], **Yuan-Xiang Tao**[a,b,†]

[a]Department of Anesthesiology, New Jersey Medical School, Rutgers, The State University of New Jersey, Newark, NJ 07103, USA

[b]Departments of Cell Biology & Molecular Medicine and Physiology, Pharmacology & Neuroscience, New Jersey Medical School, Rutgers, The State University of New Jersey, Newark, NJ 07103, USA

Keywords

E74-like factor 1; MMP9; Dorsal root ganglion; Neuropathic pain; Nerve trauma

1. Introduction

Nerve injury-caused neuropathic pain is a complex and debilitating public health crisis affecting 6.9–10% of the population around the world. Over 100 billion dollars each year are expended on neuropathic pain-related healthcare and lost productivity in the United States alone.[7] Although several strategies including anticonvulsants, antidepressants and opioids have been used in the management of this disorder, most of the patients do not achieve sufficient pain relief and/or complain of severe side effects.[44] Neuropathic pain in clinic is characterized by spontaneous pain or intermittent burning pain, enhanced pain from noxious stimuli (hyperalgesia) and pain due to innocuous stimuli (allodynia).[2] These nociceptive hypersensitivities are considered to be caused by the dysregulation of pain-associated genes at the levels of transcription and translation in primary afferent neurons of dorsal root ganglion (DRG).[18;21;25;31;48;56;57] Therefore, understanding the mechanisms of how these genes are altered may open a new door for therapeutic treatments of neuropathic pain.

[†]**Corresponding author:** Dr. Yuan-Xiang Tao, Department of Anesthesiology, New Jersey Medical School, Rutgers, The State University of New Jersey, 185 S. Orange Ave., MSB, F-661, Newark, NJ 07103. Tel: +1-973-972-9812; Fax: +1-973-972-1644. yuanxiang.tao@njms.rutgers.edu.

[*]These authors equally contributed to this work.

Author contributions

Y.X.T. conceived the project and supervised all experiments. L.Z., X.F., and Y.X.T. designed the project. L.Z., X.F., S.D. and C.H. performed the animal model, conducted behavioral experiments, and carried out microinjection, DRG culture, Western blot, chromatin immunoprecipitation, and PCR experiments. X.F. and S.W. constructed and packaged AAV5. L.Z., X.F., A.A., A.B. and Y.X.T. analyzed the data. L.Z. and Y.X.T. wrote the manuscript. All of the authors read and discussed the manuscript.

Competing Interests

The authors declare no competing interests.

Matrix metalloproteinases (MMPs), a family of calcium-dependent zinc-containing endoproteases, play a crucial role in neuroinflammation and participate in several neurological diseases including neuropathic pain through cleaving the chemokines, cytokines and extracellular matrix proteins.[52] MMP9, one of the best-studied family members is highly inducible and expressed in DRG neurons.[12] An early study showed MMP9 upregulation in injured DRG during early time period (e.g., day 1) after spinal nerve ligation (SNL).[14] Several later investigations also demonstrated significant increases in the amounts of *Mmp9* mRNA and MMP9 protein in injured DRG from day 7 to at least day 30 after SNL or chronic constriction injection (CCI) of sciatic nerve.[11;13;17;33;34;51] Epineurial, oral, intrathecal or intraperitoneal administrations of the MMP9 inhibitors attenuated the development and maintenance of mechanical allodynia caused by SNL, CCI or the L5 spinal nerve crush.[14;16;40] Intrthecal MMP9 siRNA also reduced the SNL-induced mechanical allodynia.[14] MMP9 knockout mice displayed impaired mechanical allodynia after SNL and sciatic nerve crush.[14;16] Conversely, intrathecal application of exogenous MMP9 produced neuropathic pain-like symptoms.[14] Thus, MMP9 likely is a crucial player in neuropathic pain. However, how MMP9 is increased in injured DRG following peripheral nerve injury is still elusive.

E74-like factor 1(ELF1), one of the E26 transformation-specific (ETS) transcription family members, triggers gene transcription through binding to the gene promoter or enhancer.[30;49] ELF1 is expressed in many kinds of tumor cells and promotes tumor cell invasion and migration.[38] Whether ELF1 contributes to peripheral nerve trauma-caused neuropathic pain is still elusive. The present study first examined the changes in the levels of *Elf1* mRNA and ELF1 protein in the DRG in a well-characterized mouse models of nerve trauma-induced neuropathic pain caused by CCI or SNL. We then determined whether DRG ELF1 participated in the induction and maintenance of CCI-induced mechanical and thermal hypersensitivities. Finally, we elucidated the underlying mechanism by which DRG ELF1 contributed to nerve trauma-induced neuropathic hypersensitivity.

2. Materials and methods

2.1. Animal preparations

CD1 male and female mice (approximate 7–8 weeks, weighed 20–25g) were obtained from Charles River Laboratories (Wilmington, MA). Mice were maintained in an animal room at 23 ± 2°C under an automatic 12 h light/dark cycle and provided with food and water as desired. To reduce the variability within individual mice in behavioral tests, we acclimatized the mice for ≥ 2 days before behavioral experiments. Mice were randomly grouped. The group assignment and treatment condition were blinded to the experimenters. The experimental procedures conducted were approved by the Animal Care and Use Committee of Rutgers New Jersey Medical School, in accordance with the ethical guidelines of the International Pain Research Association and the National Institutes of Health.

2.2. Neuropathic pain models

CCI- or SNL-induced neuropathic pain model in mice was established as reported previously.[18;31;55;56] The corresponding sham surgery was carried out. [18;31;55;56]

2.3. DRG microinjection

DRG microinjection was performed 14 or 35 days prior to CCI or sham surgery according to our previous studies.[8;47] In brief, after removal of L3/4 articular processes, the corresponding L3/4 DRGs were exposed. AAV5 (1 μL/DRG, 4–5 × 10^{12}) was microinjected into the exposed DRGs through a glass micropipette (tip diameter 20–40μm) connected to a Hamilton syringe using a dissection microscopy. the micropipette was pulled out 10 minutes after microinjection. All microinjected mice showed normal locomotor activities and were included in the experiments.

2.4. Behavioral tests

Mechanical, thermal and cold tests was carried out in order with 30- to 60-minute interval (back to the cages with food and water) between two tests. About 8–10 mice were tested each time.

Mechanical test was performed as described previously.[31;53;55] Two calibrated von Frey filaments (0.07 and 0.4g, Stoelting Co.) were applied for mechanical stimuli. Each application to the middle of plantar surface of one hind paw was taken for one second. Ten-trial applications (with 2–3 min intervals) per filament were carried out on one side of hind paws per mouse. Paw withdrawal frequency (PWF) was calculated as following: (number of paw withdrawals/10 trials) × 100. The duration for completion of mechanical test for all mice was approximately 1 hour.

Hear test was conducted as reported previously.[31;53;55] In brief, noxious heat from a beam of light emitted form a Model 336 Analgesic Meter (IITC Life Science Inc.) was applied on the middle of the plantar surface of one hind paw. This application per mouse was repeated 3 times with 5-min intervals on one side of hind paws per mouse. Paw withdrawal latencies (PWLs) was recorded as the length of time from the start to stop of the light beam. To avoid tissue injury, a cut-off time of twenty seconds was applied. The duration for completion of thermal test for all mice needed approximately 50 min- to 1 hour.

Cold test was conducted as reported previously.[31;53;55] PWLs were defined as the duration of time from the placement of the ipsilateral hind paw on cold aluminum plate (−1~0°C) to the jumping sign with or without hind paw shaking/ licking. Three-time placements within 10-min intervals were applied for each mouse. To avoid tissue damage, twenty seconds were applied as a cut-off time. The duration for completion of cold test for all mice required approximately 50 min- to 1 hour.

Conditioned place preference (CPP) test was performed at the 8^{th} week after viral microinjection as reported previously.[31;53;55]. In brief, thirty minutes per mouse were taken for preconditioning to acclimatize the environment with full access into two chambers with distinct stripes (horizontal vs vertical) on the walls and different texture (rough vs smooth) on the floor. After preconditioning, basal time length spent on each chamber within 15 minutes was recorded. The conditional training was carried out for the following 3 days. On day 1, mouse received intrathecal injection of lidocaine (0.4 % in 5 μl saline) and saline (5 μl) within 6-hour intervals were paired with two chambers, respectively, for 30 min. On the following 2 days, injection order of lidocaine and saline was switched every day. The

detailed procedure of intrathecal injection was described below. Mice injected with lidocaine at this concentration and injected volume displayed normal locomotor activity[31;53;55]. On the final day, the time length spent in each chamber within 15 minutes was recorded for analysis of chamber preference. Difference scores were calculated as described previously.[31;53;55]

Locomotor activity tests including placing, grasping and righting reflexes, were carried out before tissue collection according to the protocols as described previously.[31;53;55] For each reflex, five trials within 5-min intervals were conducted and the counts of each normal reflex recorded.

2.5. Intrathecal injection

The mice were given intrathecal injections under unanesthetized conditions as described previously[31;53;55] to avoid the effect of anesthetic on the lidocaine' action and locomotor activity. Intrathecal injections were performed by a quick lumbar puncture with a 0.5-inch and 30-gauge needle mated to a 10-μl syringe. Briefly, after the lower back of the mouse was rubbed with 70% ethanol, the needle was injected into intervertebral space between L3 and L4 spinous processes and then moved forward approximately 0.5 cm within the vertebral column. Five microliters of solution were injected. Based on our experience, this injection was done within less than 10 seconds (usually 5 seconds). After injection, locomotor functions in injected mice were normal.

2.6. Cell culture and transfection

DRG cultured neurons were prepared based on previously described protocl.[20;22] Briefly, the DRGs from cervical to lumbar levels of the 4-week CD1 mice were harvested in cold Neurobasal medium plus 2% B-27 Supplement, 10% fetal bovine serum, 100 units/ml penicillin, 100μg/ml streptomycin and 1% L-Glutamine. The DRGs were then digested in Hanks' balanced salt solution (without Ca^{2+} and Mg^{2+}) containing 1 mg/ml collagenase type I and 5 mg/ml dispase for 20 min at 37 °C. All these regents used above were purchased from Gibco/ThermoFisher Scientific. After being centrifuged, the dissociated cells were resuspended in mixed neurobasal medium and sieved with a 70-μm cell strainer. The cells were cultured in a 5% CO_2 atmosphere at 37 °C after they were plated onto poly-D-lysine (Sigma, USA)-pre-coated six-well plates at the density of 1–1.5 × 10^6/cm^2 cells. On the second day, AAV5 virus (10~15 μl/well, titer ≥ 1× 10^{12}) was added to each well based on experiment design. The cultured neurons were collected 3 days later.

2.7. Western blotting assay

Protein extraction and Western blotting was conducted based on the protocol published previously[6;10;26;27]. To achieve enough protein, 4 L3/4 DRGs from two CCI/sham mice or 4 L4 DRGs from four SNL/sham mice on the ipsilateral or contralateral side were pooled together. DRGs or spinal cords were homogenized in the lysis buffer (1 mM phenylmethylsulfonyl fluoride, 40 μM leupeptin, 1mM DTT, 5 mM EGTA, 1 mM EDTA, 5 mM MgCl2, 250 mM sucrose and 10 mM Tris) on the ice. After centrifugation at 1,000 × g for 15 minutes at 4°C, the supernatant (membrane/cytosolic fractions) and the pellet (nuclear fraction) were harvested. The latter was further dissolved in the lysis

buffer plus 0.1% Triton X-100 and 2% sodium dodecyl sulfate. The samples (15–20 μg/sample) were heated at 99°C for 5 minutes and loaded onto a 4% stacking/7.5% separating sodium dodecyl sulfate-polyacrylamide gel (Bio-Rad Laboratories, Hercules, CA) and then electrophoretically transferred onto a polyvinylidene difluoride membrane (Bio-Rad Laboratories). The blots were incubated first at room temperature for 2 hours in the Tris buffer containing 0.1% Tween-20 plus 5% nonfat milk and then at 4°C overnight in the primary antibodies. They includes goat anti-ELF1 (1:1,000, Invitrogen), mouse anti-histone H3 (1:1,000, Santa Cruz), mouse anti-GFAP (1:1,000, Cell Signaling Technology), rabbit anti-phosphorylated extracellular signal-regulated kinase1 and 2 (p-ERK1/2) (1:2,000, Cell Signaling Technology), rabbit anti-ERK1/2 (1:1,000, Cell Signaling Technology), rabbit anti-GAPDH (1:3000, Santa Cruz), goat anti-MMP9 (1:800, R&D systems) and rabbit anti-β-actin (1:1,000, Bioss). After being washed, the blots were incubated at room temperature for 1 hour with the anti-rabbit, anti-mouse or anti-goat secondary antibody conjugated with horseradish peroxidase (1:3,000, Jackson ImmunoResearch). The signals were finally visualized by using the enhanced chemiluminescence (ECL) reagent (Bio-Rad Laboratories) and exposed by using the ChemiDoc XRS system (Bio-Rad) with Image Lab software. The intensity of the bands was measured by using Image J software. The band intensities for nucleus proteins were normalized to H3 and those for cytosol proteins were normalized to GAPDH or β-actin.

2.8. Reverse transcription-polymerase chain reaction (RT-PCR) assay

Total RNA extraction and quantitative real-time RT-PCR assay were carried out based on our previously published protocols.[6;10;26;27] To achieve enough RNA, 4 L3/4 DRGs from two CCI/sham mice or 4 L4 DRGs from four SNL/sham mice on the ipsilateral or contralateral side were pooled together. Total RNA from DRG tissues or DRG neuronal culture was extracted by using TRIzol-chloroform methods (Invitrogen) before it was treated by using an overdose of deoxyribonuclease I (New England Biolabs). RNA was then reverse-transcribed by using the oligo(dT) primers (Invitrogen/Thermo Fisher Scientific) and ThermoScript Reverse Transcriptase (Invitrogen/Thermo Fisher Scientific). cDNA (4 μl) was amplified in a Bio-Rad CFX96 real-time PCR system by using the following primers for *Elf1* mRNA (reverse: 5'-GAGACCCAGCTGATGAT-3', forward: 5'-CAGGAGGAAGCAGCA AATTC-3'), *Mmp9* mRNA (reverse: 5'-GTGGTTCAGTTGTGGTGGTG-3', forward: 5'-CATGCACTGGGCTTAGATCA-3') or *Tuba1a* (reverse: 5'- AAGCACACATTGCCACATACAA-3', forward: 5'-TGTGGATTCTGTGGAAGG CG-3'). PCR was carried out in a 20-μl reaction volume containing 20 ng of cDNA, 10 μl of SsoAdvanced Universal SYBR Green Supermix (Bio-Rad Laboratories) and 200 nM forward and reverse primers. Reaction protocol included an initial 3 min incubation at 95 °C, followed by 39 cycles of 95 °C for 30 s, 60 °C for 30 s, and 72°C for 30 s, and a final 5 min incubation at 72°C. All PCR data were normalized to an internal control *Tuba1a*, because its expression was stable after peripheral nerve injury.[6;10;26;27] Ratios of mRNA levels at different time points post-surgery to mRNA level at 0 day were calculated using the ΔCt method ($2^{-\Delta\Delta Ct}$).

2.9. Single-cell real-time RT-PCR

In brief, the freshly DRG cultured neurons from adult mice were prepared as described above. A single living small (< 25 μm), medium (25–35 μm) or large (> 35 μm) neuron was harvested in a PCR tube containing 9–10 μL of cell lysis buffer (Signosis, Sunnyvale, CA) under an inverted microscope fit with a micromanipulator and microinjector 4 h after plating. The lysis solution was aliquoted into four PCR tubes for *Elf1*, *Mmp9*, *Gapdh* and *NeuN* (a neuronal marker) mRNAs, respectively. *Gapdh* mRNA was employed as a loading control. According to the manufacturer's instructions with the single-cell real-time RT-PCR assay kit (Signosis), the RT-PCR assay was carried out. The primers except for *NeuN* mRNA (reverse: 5′-CATCCTGATACACGACCGCT-3′, forward: 5′-AGCCTGGGAACCCATATGCC-3′) and *Gapdh* mRNA (reverse: 5′-CTCGCTCCTGGAAGATGGTG-3′, forward: 5′-GGTGAAGGTCGGTGTGAACG-3′) used were described above.

2.10. Immunohistochemistry

Mice were transcardially perfused with 50–100 ml of 4% paraformaldehyde in 0.1 M phosphate buffer (PB; pH 7.4) after they were deeply anesthetized with overdose of isoflurane. The L3/4 DRGs were collected, post-fixed with same perfusion solution for 2–4 hours and cryoprotected in 30% sucrose in 0.1 M PB for 48 hours at 4°C. The tissues were cut on a cryostat at the thickness of 15 μm. All sections were pretreated with acetone for 25 minutes and incubated at 37°C for 1 hour in 0.01 M phosphate buffer saline containing 0.3% Triton X-100 and 5% normal goat serum. The sections were then incubated at 4°C overnight with primary rabbit anti-ELF1 (1:400, biorbyt) alone or with a combination of primary rabbit anti-ELF1 and biotinylated isolectin B4 (IB4, 1:100; Sigma), mouse anti-neurofilament 200 (NF200; 1:500, Sigma-Aldrich, St. Louis, MO), mouse anti-NeuN (1:50; Gene Tex, Irvine, CA), mouse anti-calcitonin gene-related peptide (CGRP, 1:50; Abcam) or mouse anti-glutamine synthetase (GS, 1:500; EMD Millipore, Burlington, MA). Appropriate conjugated secondary antibodies were used. Under a Leica DMI4000 fluorescence microscope (Leica) with DFC365 FX camera (Leica), the immunofluorescent images were captured.

2.11. Plasmid construction and virus production

Full-length *Elf1* cDNAs was achieved from mouse DRG RNA by using the primers with restriction enzymes (reverse: 5′- GCGCTCGAGTTAAAAAGAGTTGGGCTCTAG-3′, forward: 5′- TAGAAGCTTGCCACCATGGCTGCTGTTGTCCA-3′) and the SuperScript III One-Step RT-qPCR System with the Platinum Taq High Fidelity Kit (Invitrogen/Thermo-Fisher Scientific). The PCR product was inserted into the corresponding sites of the pHpa-tra-SK plasmids (University of North Carolina, Chapel Hill) to substitute enhanced GFP sequence or the multiple cloning site of the pAAV-MCS vector (Cell Biolabs, CA). The genes in the plasmids were expressed under the control of the cytomegalovirus promoter. The designed sense and antisense sequences for *Elf1* shRNA and scrambled shRNA were annealed and inserted between the BamHI and XbaI sites of pAAV-shRNA-EF1a-EYFP. AAV5 packaging was performed by using the AAVpro Purification Kit (Takara, Mountain View, CA). Virus titer was assessed by using the AAVpro® Titration Kit (Takara).

2.12. Luciferase Assay

To construct the reporter plasmid expressing *Mmp9* gene, the 1,953 bp fragment from its promoter region (containing *Elf1* binding motif) was amplified by using the following primers (reverse: gcgctcgagGGTGTAACCATAGCGGTACAAG, forward: acgggtaccGAGAGTTTTGTAGAGAGCGT]). The PCR product was ligated into the pGL3-Basic vector (Promega, Madison, WI) and verified by DNA sequencing. According to the manufacturer's instructions, the CAD cells were co-transfected with 300 ng of pGL3-Basic vector with or without the sequences of *Mmp9* promoter, 300 ng of *Elf1* overexpression plasmid and 10 ng of the pRL-TK (Promega) by using Lipofectamine 3000 (Invitrogen). The cells were harvested and lysed in passive lysis buffer 2 days after transfection. The luciferase activity was measured by using the Dual-Luciferase Reporter Assay System (Promega). The experiments were carried out in triplicate and repeated with at least 3 separate batches of culture per group. After normalization of the firefly activity to renilla activity, relative reporter activity was determined.

2.13. Chromatin immunoprecipitation (ChIP) Assay

The ChIP assay was conducted by using the EZ ChIP Kit (Upstate/EMD Millipore) as reported previously.[6;10;26;27] In brief, after the homogenate from the DRG was cross-linked and centrifuged, the pellet was harvested and dissolved in SDS lysis buffer. To shear DNA into the fragments with a mean length of 200 to 1000 nt, the lysis was sonicated. After being pre-cleaned with protein G magnetic beads, about 10% of the samples were used as the input. The remaining samples were immunoprecipitated overnight at 4 °C with rabbit anti-ELF1 antibody or control normal rabbit serum. The fragments were detected by PCR with primers (forward: 5'-AGGTAGACAGATGGCTCGGT-3'; reverse: 5'-CCCTCCAACAGACCCGAATC-3').

2.14. Statistical analysis

The data were present as mean ± SD. Statistical analysis was accomplished by using GraphPad Prism 8. The results were statistically analyzed using a one-way, two-way, or three-way ANOVA and paired or unpaired Student's *t* test and. After ANOVA revealed a significant difference, the post hoc Tukey test was used to compare the difference between two groups. Significance was defined at $P < 0.05$.

3. Results

3.1. Time-dependent increase of ELF1 expression in injured DRG following peripheral nerve trauma

To define the role of ELF1 in nerve trauma-induced neuropathic pain, we first examined whether ELF1 expression was changed in two pain-associated regions, DRG and spinal cord dorsal horn, following CCI. Consistent with previous studies,[8;31;47;55;56] CCI, but not sham surgery, produced mechanical allodynia demonstrated by significant increases in paw withdrawal frequencies in response to 0.07 g and 0.4 g von Frey filaments and heat and cold hyperalgesia evidenced by marked decreases in paw withdrawal latencies to heat and cold stimuli, respectively, on the ipsilateral (but not contralateral) side (Fig. 1A–D). These

nociceptive hypersensitivities appeared on day 3 post-CCI and persisted for at least 14 days post-CCI (Fig. 1A–D). Accompany with these behavioral changes, the expression of FLF1 mRNA and protein was time-dependently increased in injured DRG following CCI. The levels of *Flf1* mRNA in the ipsilateral L3/4 DRGs were increased by 1.5-fold ($P < 0.05$), 1.7-fold ($P < 0.01$) and 1.5-fold ($P < 0.05$) on days 3, 7 and 14 post-CCI, respectively, as compared with the corresponding sham mice (Fig. 1E). Consistently, the amounts of ELF1 protein in the ipsilateral L3/4 DRGs were elevated by 2.4-fold ($P < 0.05$), 3.2-fold ($P < 0.01$) and 2.9-fold ($P < 0.01$) on days 3, 7 and 14 post-CCI, respectively, as compared with the corresponding sham mice (Fig. 1F). Expectedly, basal expression of ELF1 was not changed in the contralateral L3/4 DRG and ipsilateral L3/4 spinal cord dorsal horn after CCI and in both ipsilateral and contralateral L3/4 DRGs after sham surgery during the observation period (Fig. 1F–G). Similar results were observed after SNL (Fig. 1H–I). The levels of total ELF1 protein in the ipsilateral L4 DRG were elevated by 2.2-fold ($P < 0.05$), 2.61-fold ($P < 0.01$) and 2.1-fold ($P < 0.01$) on days 3, 7 and 14 post-SNL, respectively, as compared with the corresponding sham mice (Fig. 1H). No changes in basal expression of ELF1 were seen in the ipsilateral L3 DRG, contralateral L4 DRG and ipsilateral L4 spinal cord dorsal horn after SNL (Fig. 1I).

We further observed the distribution pattern of ELF1 in the DRG of naïve mice. ELF1 was colocalized with the specific neuronal marker NeuN in DRG cells (Fig. 2A) and was not detected in the GS (a marker for satellite glial cell)-labelled cells (Fig. 2B). About 27.7% (101/364) of NeuN-positive cells are labeled for ELF1. A cross-sectional area assessment of neuronal somata showed that approximately 41.2% of ELF1-positive neurons were large, 38.7% were medium and 20.1% were small (Fig. 2C). A DRG subpopulation analysis showed that approximately 32.7% of ELF1-labeled cells were positive for CGRP (a marker for small DRG peptidergic neurons), 23.2% were positive by IB4 (a marker for small nonpeptidergic neurons), and 49.5% were lpositive by NF200 (a marker for medium/large neurons and myelinated Ab fibers) (Fig. 2D–F). On day 7 post-CCI, number of ELF1-positive neurons in the ipsilateral L4 DRG was 1.66-fold of the value in the contralateral L4 DRG ($P < 0.01$; Fig. 2H).

3.2. Effect of preventing increased DRG ELF1 on the development of CCI-induced nociceptive hypersensitivity

Next, we investigated whether the increased ELF1 in injured DRG contributed to the development of neuropathic mechanical and thermal hypersensitivity. To block this increase, we microinjected AAV5 expressing *Elf1* shRNA (AAV5-*Elf1* shRNA) into the ipsilateral L3/4 DRGs of male mice 35 days before CCI or sham surgery, as AAV5 requires 3–4 weeks to become expressed.[18;31;56;57] AAV5 expressing control scrambled shRNA (AAV5-*Scr* shRNA) was used as the control. As expected, the amount of ELF1 was significantly elevated by 1.8-fold in the ipsilateral L3/4 DRGs of the AAV5-*Scr*-microinjected CCI mice, as compared to the AAV5-*Scr* shRNA-microinjected sham mice on day 14 after surgery ($P < 0.05$; Fig. 3A). This increase was not found in the AAV5-*Elf1* shRNA-microinjected CCI mice (0.96-fold of AAV5-*Scr*-sham; Fig. 3A). Neither viral microinjection changed basal level of ELF1 in the ipsilateral L3/4 DRGs of sham mice (Fig. 3A).

We further examined the behavioral responses of CCI or sham male mice after AAV5 microinjection. Similar to the observation above, mechanical allodynia and heat and cold hyperalgesia were found on the ipsilateral side from days 3 to 14 post-CCI in AAV5-*Scr* shRNA-microinjected mice (Fig. 3B–E). Microinjection of AAV5-*Elf1* shRNA substantially attenuated the CCI-induced increases in paw withdrawal frequencies to 0.07 g and 0.4 g von Frey filament stimuli ($P < 0.01$; Fig. 3B–C) and the CCI-induced decreases in paw withdrawal latencies to heat ($P < 0.01$; Fig. 3D) and cold ($P < 0.01$; Fig. 3E) stimuli from days 3 to 14 post-surgery. DRG microinjection of neither virus changed basal responses on the contralateral side of CCI mice and on either side of sham mice during the examination period (Fig. 3B–H). All microinjected mice exhibited normal locomotor function (Table 1). The results were similar after DRG viral microinjection in female CCI/sham mice (Fig. S1A–H).

We also observed whether DRG microinjection of AAV5-*Elf1* shRNA affected CCI-induced central sensitization in dorsal horn, as evidenced by increases in GFAP (a marker for astrocyte hyperactivation) and p-ERK1/2 (a marker for neuronal hyperactivation) in the dorsal horn during the development period in male mice. Consistent with previous studies,[27–30] the amounts of p-ERK1/2 (but not total ERK1/2) and GFAP were elevated in the ipsilateral L3/4 dorsal horn on day 14 post-CCI in the AAV5-*Scr* shRNA-microinjected CCI mice ($P < 0.01$; Fig. 3I). These increases were not oberved in the AAV5-*Elf1* shRNA-microinjected CCI mice ($P < 0.01$; Fig. 3I). Neither virus altered basal amounts of total ERK1/2, p-ERK1/2 or GFAP in the ipsilateral L3/4 dorsal horn of sham mice (Fig. 3I). Similar changes were found in female CCI/sham mice after DRG viral microinjection (Fig. S1I)

Taken together, these findings suggest that increased ELF1 in injured DRG is required for induction of CCI-induced nociceptive hypersensitivity and dorsal horn central sensitization.

3.3. Effect of blocking increased DRG ELF1 on the maintenance of CCI-induced nociceptive hypersensitivity

To examine the role of increased DRG ELF1 in the maintenance of CCI-caused nociceptive hypersensitivity, we microinjected AAV5-*Elf1* shRNA 14 days before CCI in male mice. Ipsilateral mechanical allodynia and heat and cold hyperalgesia were completely developed on day 7 post-CCI in both AAV5-*Elf1* shRNA- and AAV5-*Scr* shRNA-microinjected mice ($P < 0.01$, Day 7 *vs* Day −1; Fig. 4A–D). However, these nociceptive hypersensitivities were decreased in the AAV5-*Elf1* shRNA-microinjected mice on days 14, 21 and 28 post-CCI ($P < 0.05$ or 0.01, AAV5-*Elf1* shRNA-CCI *vs* AAV5-*Scr* shRNA-CCI; Fig. 4A–D). Basal responses to mechanical, heat and cold stimuli were not changed on the contralateral side of AAV5-microinjected CCI mice (Fig. 4E–G). As expected, CCI elevated the expression of ELF1 protein by 2.2-fold in the ipsilateral L3/4 DRGs on day 28 post-CCI in the AAV5-*Scr* shRNA-microinjected mice as compared with naive L3/4 DRGs ($P < 0.05$; Fig. 4H), but this elevation was entirely absent in the AAV5-*Elf1* shRNA-microinjected CCI mice ($P < 0.05$, AAV5-*Elf1* shRNA-CCI *vs* AAV5-*Scr* shRNA-CCI; Fig. 4H). In addition, CCI-induced increases in GFAP and p-ERK1/2 (but not total ERK1/2) in the ipsilateral L3/4 dorsal horn on day 28 post-CCI from the AAV5-*Scr* shRNA-microinjected mice were

not seen in the AAV5-*Elf1* shRNA-microinjected mice ($P < 0.01$, AAV5-*Elf1* shRNA-CCI *vs* AAV5-*Scr* shRNA-CCI; Fig. 4I). These results indicate that increased DRG ELF1 is also critical in the maintenance of CCI-induced nociceptive hypersensitivity and dorsal horn central sensitization.

3.4. Effect of DRG ELF1 overexpression on nociceptive thresholds in naïve mice

We further determined whether the increased DRG ELF1 was sufficient for nerve trauma-induced nociceptive hypersensitivity. To this end, AAV5 that expresses mouse full-length *Elf1* mRNA (AAV5-*Elf1*) was microinjected into unilateral L3/4 DRGs of naïve male mice. AAV5 encoding green fluorescent protein (AAV5-*Gfp*) was employed as a control. DRG microinjection of AAV5-*Elf1*, but not AAV5-*Gfp*, produced significant increases in paw withdrawal frequencies in response to 0.07 g and 0.4 g von Frey filament stimuli ($P < 0.01$, AAV5-*Elf1 vs* AAV5-*Gfp*; Fig. 5A–B) and reductions in paw withdrawal latencies in response to heat and cold stimuli ($P < 0.01$, AAV5-*Elf1 vs* AAV5-*Gfp*; Fig. 5C–D) from week 5 to at least week 9 after microinjection on the ipsilateral side. Neither virus altered basal responses on the contralateral side (Fig. 5A–D) and locomotor function (Table 1). Besides evoked nociceptive hypersensitivity, DRG microinjection of AAV5-*Elf1* produced evoked stimulation-independent nociceptive hypersensitivity evidenced by marked preference for the lidocaine-paired chamber on week 8 after microinjection ($P < 0.01$, AAV5-*Elf1 vs* AAV5-*Gfp*; Fig. 5E–F).As expected, DRG microinjection of AAV5-*Gfp* did not lead to significant preference for either saline- or lidocaine-paired chamber, indicating no spontaneous pain (Fig. 5E–F). The level of ELF1 protein was elevated by 2.9-fold in the AAV5-*Elf1*-microinjected DRGs as compared with AAV5-*Gfp*-microinjected DRGs 9 weeks after microinjection ($P < 0.05$; Fig. 5G). DRG microinjection of AAV5-*Elf1*, but AAV5-*Gfp*, also increased the amounts of GFAP and p-ERK1/2 (but not total ERK1/2) in the ipsilateral L3/4 dorsal horn 9 weeks after microinjection ($P < 0.01$, AAV5-*Elf1 vs* AAV5-*Gfp*; Fig. 5H). Similar findings were seen after DRG microinjection of AAV5-*Elf1* or AAV5-*Gfp* in naive female mice (Fig. S2A–H). Taken together, our findings suggest that mimicking the CCI-induced increase in DRG ELF1 produces both spontaneous and evoked pain hypersensitivities.

3.5. Participation of increased ELF1 in CCI-induced upregulation of MMP9 in injured DRG

We finally explored the mechanisms by which increased ELF1 in injured DRG contributed to CCI-induced nociceptive hypersensitivity. We used the online software TFBS (http://tfbsdb.systemsbiology.net/) and identified a consensus *Elf1* binding site within the distal promoter region of the *Mmp9* gene. This binding site was also predicted in abdominal aortic aneurysm tissue.[29] Given that nerve trauma-induced MMP9 upregulation in injured DRG participated in neuropathic hypersensitivity,[11;13;14;16;17;33;34;40;51] we proposed that increased ELF1 may be involved in this upregulation. Consistent with previous studies,[11;12;33;34;51] CCI upregulated MMP9 expression in the ipsilateral L3/4 DRGs on days 14 ($P < 0.01$, CCI *vs* sham in AAV5-*Scr* shRNA mice; Fig. 6A) and 28 ($P < 0.01$, CCI in AAV5-*Scr* shRNA mice *vs* naive mice; Fig. 6B) post-CCI in the AAV5-*Scr* shRNA-microinjected mice. These upregulations were largely blocked in the AAV5-*Elf1* shRNA-microinjected CCI mice ($P < 0.01$, AAV5-*Elf1* shRNA *vs* AAV5-*Scr* shRNA in CCI mice or on the ipsilateral side; Fig. 6A–B). DRG microinjection of AAV5-*Elf1* shRNA did not

significantly reduce basal level of MMP9 in the ipsilateral L3/4 DRGs of sham mice (Fig. 6A). Consistently, the amount of MMP9 in the ipsilateral L3/4DRGs of the AAV5-*Elf1*-microinjected mice was increased by 2.9-fold as compared with AAV5-*Gfp*-microinjeced mice 9 weeks post-microinjection ($P < 0.01$, AAV5-*Elf1 vs* AAV5-*Gfp*; Fig. 6C). In *in vitro* DRG neuronal culture, co-transduction of AAV5-*Elf1* plus AAV5-*Scr* shRNA increased the levels of not only *Elf1* mRNA but also *Mmp9* mRNA ($P < 0.05$ or 0.01, AAV5-*Elf1 vs* AAV5-*Gfp* in AAV5-*Scr* shRNA-treated culture; Fig. 6D). These increases were absent in cultured DRG neurons co-transduced with AAV5-*Elf1* plus AAV5-*Elf1* shRNA ($P < 0.05$ or 0.01, AAV5-*Elf1* shRNA *vs* AAV5-*Scr* shRNA in AAV5-*Elf1*-treated culture; Fig. 6D). Furthermore, the luciferase assay showed that co-transduction of full-length *Elf1* vector (but not control *Gfp* vector) with *Mmp9* reporter vector markedly elevated the activity of the *Mmp9 p*romoter in *in vitro* CAD cells ($P < 0.01$, *Elf1 vs Gfp*; Fig. 6E). ChIP assay showed that the fragment of the *Mmp9* promoter including the *Elf1* binding motif could be amplified from the complex immunoprecipitated with ELF1 antibody in nuclear fraction from L3/4 DRGs of sham mice (Fig. 6F). CCI increased the binding of ELF1 to *Mmp9* promoter, as indicated by a 1.8-fold increase in binding activity in the ipsilateral L3/4 DRGs on day 14 post-CCI ($P < 0.01$, CCI *vs* sham; Fig. 6F). Finally, single cell RT-PCR assay revealed that *Elf1* mRNA co-expressed with *Mmp9* mRNA in individual large, medium and small DRG neurons (Fig. 6G). These findings suggest that increased ELF1 contributed to CCI-induced nociceptive hypersensitivity through upregulating MMP9 in injured DRG.

4. Discussion

CCI-induced peripheral nerve trauma produces chronic nociceptive hypersensitivities including spontaneous pain, mechanical allodynia and heat and cold hyperalgesia in the preclinical animal models, similar to the symptoms in peripheral nerve trauma-caused neuropathic pain often occurring after thoracotomy, breast surgery, cardiac surgery and limb amputation in the clinic. Understanding how CCI leads to nociceptive hypersensitivity may open new doors for neuropathic pain managements. Present study showed that CCI/SNL led to an elevation in ELF1 expression in injured DRG. This elevation contributed to the development and maintenance of CCI-induced nociceptive hypersensitivity through upregulation of MMP9 in injured DRG. Our results suggest that ELF1 is a potential target for therapeutic treatment of nerve trauma-induced neuropathic pain.

Similar to other transcription factors such as runt-related transcription factor 1,[18] octamer transcription factor 1[54;56] and myeloid zinc finger,[19;57] ELF1 expression can be regulated in the DRG following peripheral nerve trauma. The present work showed that CCI or SNL produced the marked and time-dependent elevations of *Elf1* mRNA and ELF1 protein in injured DRG. Both models are complementary as SNL-induced nociceptive hypersensitivity results mainly from direct nerve injury, whereas CCI-induced nociceptive hypersensitivity is initiated primarily by ischemia.[1;15;32] These increases likely occur in majority of medium and large diameter neurons of injured DRG because ELF1 is distributed predominantly in these DRG neurons under normal conditions. Given that these increases were correlated to the development and maintenance of nerve trauma-induced nociceptive hypersensitivity and that involvement of large- and medium-diameter DRG neurons in neuropathic pain genesis is well documented. [4;23;24;39;42;45] our findings suggest that

the elevated ELF1 in injured DRG may be implicated in neuropathic pain (Fig. 7). Our findings also indicate that *Elf1* gene is transcriptionally activated after peripheral nerve trauma. Although the detailed mechanisms of how nerve trauma elevates the *Ebf1* mRNA expression in injured DRG are still elusive, this activation may be caused by epigenetic modifications and/or increases in RNA stability [3;28;46] as well as related to other transcription factors. These possibilities will be examined in our future work.

In the present study, we carried out the AAV5-*Elf1* shRNA strategy to examine the role of DRG ELF1 in CCI-induced nociceptive hypersensitivity. We reported that microinjection of AAV5-*Elf1* shRNA into injured DRG blocked the CCI-induced elevation of DRG ELF1 and nociceptive hypersensitivity. Given that AAV5-*Elf1* shRNA did not impact acute/basal pain and locomotor functions, this strongly indicates the specificity and selectivity of AAV5-*Elf1* shRNA effect. Unexpectedly, DRG microinjection of AAV5-*Elf1* shRNA failed to markedly knock down basal level of ELF1 in the sham DRG. Transduction of AAV5-*Elf1* shRNA into *in vitro* DRG neuronal culture also did not significantly alter basal level of *Elf1* mRNA expression. The reason of why AAV5-*Elf1* shRNA did not impact basal ELF1 expression is unclear, but it is very likely that its lower basal expression in DRG under normal conditions cannot be further knocked down significantly by AAV5-*Elf1* shRNA at the present dosage used.

The increased ELF1 in injured DRG contributes to the CCI-induced nociceptive hypersensitivity through upregulating MMP9 expression in injured DRG (Fig. 7). MMP9, an endoprotease, participates in nerve trauma-induced nociceptive hypersensitivity through interleukin-1β cleavage in injured DRG (Fig. 7).[14] One early study reported MMP9 upregulation in injured DRG at early time points (e.g., on day 1) after SNL.[14] Several later studies also revealed that the levels of *Mmp9* mRNA and MMP9 protein were markedly increased in injured DRG on days 7, 14 and 30 post-CCI or SNL. [11;12;33;34;51] Consistent with these studies, the present study also revealed robust upregulation of MMP9 protein in the ipsilateral L3/4 DRGs on days 14 and 28 post-CCI. Persistent intrathecal infusion of an MMP9 inhibitor for 5 days starting before SNL produced an anti-nociceptive effect that lasted for at least 11 days after SNL.[14] Knockdown or knockout of DRG MMP9 also reduced SNL-induced mechanical allodynia. [14;16] Thus, increased DRG MMP9 might be an endogenous irritator of neuropathic pain (Fig. 7). Our findings showed that ELF1 transcriptionally activated *Mmp9* gene in injured DRG after CCI. DRG microinjection of AAV5-*Elf1* shRNA blocked not only the CCI-induced nociceptive hypersensitivity bust also the CCI-induced increase in DRG MMP9 of both male and female mice. Conversely, DRG overexpression of AAV5-*Elf1* upregulated basal expression of DRG MMP5 and produced both stimulation-dependent and -independent nociceptive hypersensitivities (although the stimulation-independent nociceptive hypersensitivity possibly caused by the procedure of intrathecal injection could not be excluded) in both male and female mice. Moreover, the binding activity of ELF1 to the *Mmp9* promoter was markedly elevated in injured DRG after CCI. *In vitro* experiment revealed direct activation of *Mmp9* promoter activity by ELF1 overexpression. Given that *Elf1* mRNA and *Mmp9* mRNA co-existed in individual DRG neurons and that IL-1β is essential for sensitization of DRG neurons (Fig. 7),[14;36;41] the antinociceptive effect caused by preventing the CCI-induced elevation of DRG ELF1 possibly results from

the failure to transcriptionally activate *Mmp9* gene in injured DRG after CCI (Fig. 7). Without an elevation in MMP9 protein, no alternations would occur in the increase of the cleaved forms of IL-1β and its triggered neuronal sensitization in injured DRG (Fig. 7), and subsequent central sensitization in the ipsilateral dorsal horn. Indeed, blocking the CCI-induced increase in DRG ELF1 abolished the CCI-induced increases in markers for hyperactivation in dorsal horn neurons and astrocytes. We conclude that DRG ELF1 participates in neuropathic hypersensitivity at least in part through the MMP9-mediated mechanism (Fig. 7). It should be worth noting that other potential mechanisms by which increased DRG ELF1 contributes to neuropathic pain cannot be excluded. Besides MMP9, ELF1 may transcriptionally regulate the expression of other transcription factors (e.g., activating transcription factor 5) and other downstream signals (e.g., human Pygopus 2).[5;9;43] Whether these potential downstream targets mediate the function of ELF1 in neuropathic pain remains to be determined, but targeting ELF1 through blocking these multiple downstream signals likely produces more highly efficient antinociception as compared to targeting its downstream signal (e.g., MMP9) alone or even current medication such as gabapentin.

In conclusion, we identified an ELF1-triggered transcriptional mechanism by which nerve trauma upregulates DRG MMP9 expression. Because preventing elevated DRG ELF1 alleviates nerve trauma-induced nociceptive hypersensitivities without altering acute/basal pain and locomotor function, ELF1 may be a key initiator of neuropathic pian and a potential new target for treatment of this disorder. Although shRNA strategy used in the present study has not been applied in clinic practice, intrathecal delivery of the chemically modified long-acting antisense oligonucleotides have been approved by the FDA for clinical therapy.[35;37;50] In our future studies, we will designed the modified antisense oligonucleotide specifically targeting ELF1 and observe its role in nerve trauma-induced nociceptive hypersensitivity. Nevertheless, potential unwanted effects caused by targeting ELF1 should be paid an attention because of its expression widely in body tissues.

Supplementary Material

Refer to Web version on PubMed Central for supplementary material.

Acknowledgements

This work was supported by grant (RFNS113881) from the National Institutes of Health (Bethesda, Maryland, USA).

References

[1]. Bennett GJ, Xie YK. A peripheral mononeuropathy in rat that produces disorders of pain sensation like those seen in man. Pain 1988;33:87–107. [PubMed: 2837713]

[2]. Campbell JN, Meyer RA. Mechanisms of neuropathic pain. Neuron 2006;52:77–92. [PubMed: 17015228]

[3]. Chatterjee B, Shen CJ, Majumder P. RNA Modifications and RNA Metabolism in Neurological Disease Pathogenesis. Int J Mol Sci 2021;22.

[4]. Devor M Ectopic discharge in Abeta afferents as a source of neuropathic pain. Exp Brain Res 2009;196:115–128. [PubMed: 19242687]

[5]. Duan H, He H, Hu Q, Lin Y, Cao S, Lan X, Li L, Pang D. Comparison of regulatory networks of E74-like factor 1 and cold-shock domain-containing E1 in breast cancer cell lines using ChIP datasets. Exp Ther Med 2020;20:245. [PubMed: 33178343]

[6]. Fu G, Du S, Huang T, Cao M, Feng X, Wu S, Albik S, Bekker A, Tao YX. FTO (Fat-Mass and Obesity-Associated Protein) Participates in Hemorrhage-Induced Thalamic Pain by Stabilizing Toll-Like Receptor 4 Expression in Thalamic Neurons. Stroke 2021;52:2393–2403. [PubMed: 34102854]

[7]. Gaskin DJ, Richard P. The economic costs of pain in the United States. J Pain 2012;13:715–724. [PubMed: 22607834]

[8]. He L, Han G, Wu S, Du S, Zhang Y, Liu W, Jiang B, Zhang L, Xia S, Jia S, Hannaford S, Xu Y, Tao YX. Toll-like receptor 7 contributes to neuropathic pain by activating NF-kappaB in primary sensory neurons. Brain Behav Immun 2020;87:840–851. [PubMed: 32205121]

[9]. Hu M, Li H, Xie H, Fan M, Wang J, Zhang N, Ma J, Che S. ELF1 Transcription Factor Enhances the Progression of Glioma via ATF5 promoter. ACS Chem Neurosci 2021;12:1252–1261. [PubMed: 33720698]

[10]. Huang T, Fu G, Gao J, Zhang Y, Cai W, Wu S, Jia S, Xia S, Bachmann T, Bekker A, Tao YX. Fgr contributes to hemorrhage-induced thalamic pain by activating NF-kappaB/ERK1/2 pathways. JCI Insight 2020;5.

[11]. Ito T, Sakai A, Maruyama M, Miyagawa Y, Okada T, Fukayama H, Suzuki H. Dorsal Root Ganglia Homeobox downregulation in primary sensory neurons contributes to neuropathic pain in rats. Mol Pain 2020;16:1744806920904462.

[12]. Jurga AM, Piotrowska A, Makuch W, Przewlocka B, Mika J. Blockade of P2X4 Receptors Inhibits Neuropathic Pain-Related Behavior by Preventing MMP-9 Activation and, Consequently, Pronociceptive Interleukin Release in a Rat Model. Front Pharmacol 2017;8:48. [PubMed: 28275350]

[13]. Jurga AM, Rojewska E, Piotrowska A, Makuch W, Pilat D, Przewlocka B, Mika J. Blockade of Toll-Like Receptors (TLR2, TLR4) Attenuates Pain and Potentiates Buprenorphine Analgesia in a Rat Neuropathic Pain Model. Neural Plast 2016;2016:5238730. [PubMed: 26962463]

[14]. Kawasaki Y, Xu ZZ, Wang X, Park JY, Zhuang ZY, Tan PH, Gao YJ, Roy K, Corfas G, Lo EH, Ji RR. Distinct roles of matrix metalloproteases in the early- and late-phase development of neuropathic pain. Nat Med 2008;14:331–336. [PubMed: 18264108]

[15]. Kim SH, Chung JM. An experimental model for peripheral neuropathy produced by segmental spinal nerve ligation in the rat. Pain 1992;50:355–363. [PubMed: 1333581]

[16]. Kobayashi H, Chattopadhyay S, Kato K, Dolkas J, Kikuchi S, Myers RR, Shubayev VI. MMPs initiate Schwann cell-mediated MBP degradation and mechanical nociception after nerve damage. Mol Cell Neurosci 2008;39:619–627. [PubMed: 18817874]

[17]. Kwan MY, Choo A, Hanania T, Ghavami A, Beltran J, Shea J, Barboza A, Hu A, Fowler M, Neelagiri VR, Sucholeiki I. Biomarker Analysis of Orally Dosed, Dual Active, Matrix Metalloproteinase (MMP)-2 and MMP-9 Inhibitor, AQU-118, in the Spinal Nerve Ligation (SNL) Rat Model of Neuropathic Pain. Int J Mol Sci 2019;20.

[18]. Li Y, Guo X, Sun L, Xiao J, Su S, Du S, Li Z, Wu S, Liu W, Mo K, Xia S, Chang YJ, Denis D, Tao YX. N(6)-Methyladenosine Demethylase FTO Contributes to Neuropathic Pain by Stabilizing G9a Expression in Primary Sensory Neurons. Adv Sci (Weinh) 2020;7:1902402. [PubMed: 32670741]

[19]. Li Z, Gu X, Sun L, Wu S, Liang L, Cao J, Lutz BM, Bekker A, Zhang W, Tao YX. Dorsal root ganglion myeloid zinc finger protein 1 contributes to neuropathic pain after peripheral nerve trauma. Pain 2015;156:711–721. [PubMed: 25630025]

[20]. Liang L, Gu X, Zhao JY, Wu S, Miao X, Xiao J, Mo K, Zhang J, Lutz BM, Bekker A, Tao YX. G9a participates in nerve injury-induced Kcna2 downregulation in primary sensory neurons. Sci Rep 2016;6:37704. [PubMed: 27874088]

[21]. Liang L, Lutz BM, Bekker A, Tao YX. Epigenetic regulation of chronic pain. Epigenomics 2015;7:235–245. [PubMed: 25942533]

[22]. Liang L, Zhao JY, Gu X, Wu S, Mo K, Xiong M, Bekker A, Tao YX. G9a inhibits CREB-triggered expression of mu opioid receptor in primary sensory neurons following peripheral nerve injury. Mol Pain 2016;12:1–16.

[23]. Liu CN, Michaelis M, Amir R, Devor M. Spinal nerve injury enhances subthreshold membrane potential oscillations in DRG neurons: relation to neuropathic pain. J Neurophysiol 2000;84:205–215. [PubMed: 10899197]

[24]. Liu CN, Wall PD, Ben-Dor E, Michaelis M, Amir R, Devor M. Tactile allodynia in the absence of C-fiber activation: altered firing properties of DRG neurons following spinal nerve injury. Pain 2000;85:503–521. [PubMed: 10781925]

[25]. Lutz BM, Bekker A, Tao YX. Noncoding RNAs: new players in chronic pain. Anesthesiology 2014;121:409–417. [PubMed: 24739997]

[26]. Lutz BM, Wu S, Gu X, Atianjoh FE, Li Z, Fox BM, Pollock DM, Tao YX. Endothelin type A receptors mediate pain in a mouse model of sickle cell disease. Haematologica 2018;103:1124–1135. [PubMed: 29545351]

[27]. Mao Q, Wu S, Gu X, Du S, Mo K, Sun L, Cao J, Bekker A, Chen L, Tao YX. DNMT3a-triggered downregulation of K2p 1.1 gene in primary sensory neurons contributes to paclitaxel-induced neuropathic pain. Int J Cancer 2019.

[28]. Mehler MF. Epigenetic principles and mechanisms underlying nervous system functions in health and disease. Prog Neurobiol 2008;86:305–341. [PubMed: 18940229]

[29]. Nischan J, Gatalica Z, Curtis M, Lenk GM, Tromp G, Kuivaniemi H. Binding sites for ETS family of transcription factors dominate the promoter regions of differentially expressed genes in abdominal aortic aneurysms. Circ Cardiovasc Genet 2009;2:565–572. [PubMed: 20031636]

[30]. Oettgen P, Akbarali Y, Boltax J, Best J, Kunsch C, Libermann TA. Characterization of NERF, a novel transcription factor related to the Ets factor ELF-1. Mol Cell Biol 1996;16:5091–5106. [PubMed: 8756667]

[31]. Pan Z, Du S, Wang K, Guo X, Mao Q, Feng X, Huang L, Wu S, Hou B, Chang YJ, Liu T, Chen T, Li H, Bachmann T, Bekker A, Hu H, Tao YX. Downregulation of a Dorsal Root Ganglion-Specifically Enriched Long Noncoding RNA is Required for Neuropathic Pain by Negatively Regulating RALY-Triggered Ehmt2 Expression. Adv Sci (Weinh) 2021;8:e2004515. [PubMed: 34383386]

[32]. Rigaud M, Gemes G, Barabas ME, Chernoff DI, Abram SE, Stucky CL, Hogan QH. Species and strain differences in rodent sciatic nerve anatomy: implications for studies of neuropathic pain. Pain 2008;136:188–201. [PubMed: 18316160]

[33]. Rojewska E, Makuch W, Przewlocka B, Mika J. Minocycline prevents dynorphin-induced neurotoxicity during neuropathic pain in rats. Neuropharmacology 2014;86:301–310. [PubMed: 25172308]

[34]. Rojewska E, Popiolek-Barczyk K, Jurga AM, Makuch W, Przewlocka B, Mika J. Involvement of pro- and antinociceptive factors in minocycline analgesia in rat neuropathic pain model. J Neuroimmunol 2014;277:57–66. [PubMed: 25304927]

[35]. Roovers J, De JP, Weckhuysen S. The therapeutic potential of RNA regulation in neurological disorders. Expert Opin Ther Targets 2018;22:1017–1028. [PubMed: 30372655]

[36]. Samad TA, Moore KA, Sapirstein A, Billet S, Allchorne A, Poole S, Bonventre JV, Woolf CJ. Interleukin-1beta-mediated induction of Cox-2 in the CNS contributes to inflammatory pain hypersensitivity. Nature 2001;410:471–475. [PubMed: 11260714]

[37]. Scoles DR, Pulst SM. Oligonucleotide therapeutics in neurodegenerative diseases. RNA Biol 2018;15:707–714. [PubMed: 29560813]

[38]. Seth A, Watson DK. ETS transcription factors and their emerging roles in human cancer. Eur J Cancer 2005;41:2462–2478. [PubMed: 16213704]

[39]. Sittl R, Lampert A, Huth T, Schuy ET, Link AS, Fleckenstein J, Alzheimer C, Grafe P, Carr RW. Anticancer drug oxaliplatin induces acute cooling-aggravated neuropathy via sodium channel subtype Na(V)1.6-resurgent and persistent current. Proc Natl Acad Sci U S A 2012;109:6704–6709. [PubMed: 22493249]

[40]. Sommer C, Schmidt C, George A, Toyka KV. A metalloprotease-inhibitor reduces pain associated behavior in mice with experimental neuropathy. Neurosci Lett 1997;237:45–48. [PubMed: 9406876]

[41]. Sweitzer S, Martin D, DeLeo JA. Intrathecal interleukin-1 receptor antagonist in combination with soluble tumor necrosis factor receptor exhibits an anti-allodynic action in a rat model of neuropathic pain. Neuroscience 2001;103:529–539. [PubMed: 11246166]

[42]. Tal M, Wall PD, Devor M. Myelinated afferent fiber types that become spontaneously active and mechanosensitive following nerve transection in the rat. Brain Res 1999;824:218–223. [PubMed: 10196451]

[43]. Tzenov YR, Andrews PG, Voisey K, Popadiuk P, Xiong J, Popadiuk C, Kao KR. Human papilloma virus (HPV) E7-mediated attenuation of retinoblastoma (Rb) induces hPygopus2 expression via Elf-1 in cervical cancer. Mol Cancer Res 2013;11:19–30. [PubMed: 23284001]

[44]. Vorobeychik Y, Gordin V, Mao J, Chen L. Combination therapy for neuropathic pain: a review of current evidence. CNS Drugs 2011;25:1023–1034. [PubMed: 22133325]

[45]. Weissner W, Winterson BJ, Stuart-Tilley A, Devor M, Bove GM. Time course of substance P expression in dorsal root ganglia following complete spinal nerve transection. J Comp Neurol 2006;497:78–87. [PubMed: 16680762]

[46]. Weskamp K, Barmada SJ. RNA Degradation in Neurodegenerative Disease. Adv Neurobiol 2018;20:103–142. [PubMed: 29916018]

[47]. Wu Q, Wei G, Ji F, Jia S, Wu S, Guo X, He L, Pan Z, Miao X, Mao Q, Yang Y, Cao M, Tao YX. TET1 Overexpression Mitigates Neuropathic Pain Through Rescuing the Expression of mu-Opioid Receptor and Kv1.2 in the Primary Sensory Neurons. Neurotherapeutics 2019;16:491–504. [PubMed: 30515739]

[48]. Wu S, Bono J, Tao YX. Long noncoding RNA (lncRNA): A target in neuropathic pain. Expert Opin Ther Targets 2018.

[49]. Wurster AL, Siu G, Leiden JM, Hedrick SM. Elf-1 binds to a critical element in a second CD4 enhancer. Mol Cell Biol 1994;14:6452–6463. [PubMed: 7935370]

[50]. Wurster CD, Ludolph AC. Antisense oligonucleotides in neurological disorders. Ther Adv Neurol Disord 2018;11:1756286418776932.

[51]. Yang CH, Yip HK, Chen HF, Yin TC, Chiang JY, Sung PH, Lin KC, Tsou YH, Chen YL, Li YC, Huang TH, Huang CR, Luo CW, Chen KH. Long-term Therapeutic Effects of Extracorporeal Shock Wave-Assisted Melatonin Therapy on Mononeuropathic Pain in Rats. Neurochem Res 2019;44:796–810. [PubMed: 30632086]

[52]. Yang Y, Hill JW, Rosenberg GA. Multiple roles of metalloproteinases in neurological disorders. Prog Mol Biol Transl Sci 2011;99:241–263. [PubMed: 21238938]

[53]. Yang Y, Wen J, Zheng B, Wu S, Mao Q, Liang L, Li Z, Bachmann T, Bekker A, Tao YX. CREB Participates in Paclitaxel-Induced Neuropathic Pain Genesis Through Transcriptional Activation of Dnmt3a in Primary Sensory Neurons. Neurotherapeutics 2021;18:586–600. [PubMed: 33051852]

[54]. Yuan J, Wen J, Wu S, Mao Y, Mo K, Li Z, Su S, Gu H, Ai Y, Bekker A, Zhang W, Tao YX. Contribution of dorsal root ganglion octamer transcription factor 1 to neuropathic pain after peripheral nerve injury. Pain 2019;160:375–384. [PubMed: 30247265]

[55]. Zhang Z, Zheng B, Du S, Han G, Zhao H, Wu S, Jia S, Bachmann T, Bekker A, Tao YX. Eukaryotic initiation factor 4 gamma 2 contributes to neuropathic pain through downregulation of Kv1.2 and the mu opioid receptor in mouse primary sensory neurones. Br J Anaesth 2020.

[56]. Zhao JY, Liang L, Gu X, Li Z, Wu S, Sun L, Atianjoh FE, Feng J, Mo K, Jia S, Lutz BM, Bekker A, Nestler EJ, Tao YX. DNA methyltransferase DNMT3a contributes to neuropathic pain by repressing Kcna2 in primary afferent neurons. Nat Commun 2017;8:14712. [PubMed: 28270689]

[57]. Zhao X, Tang Z, Zhang H, Atianjoh FE, Zhao JY, Liang L, Wang W, Guan X, Kao SC, Tiwari V, Gao YJ, Hoffman PN, Cui H, Li M, Dong X, Tao YX. A long noncoding RNA contributes to neuropathic pain by silencing Kcna2 in primary afferent neurons. Nat Neurosci 2013;16:1024–1031. [PubMed: 23792947]

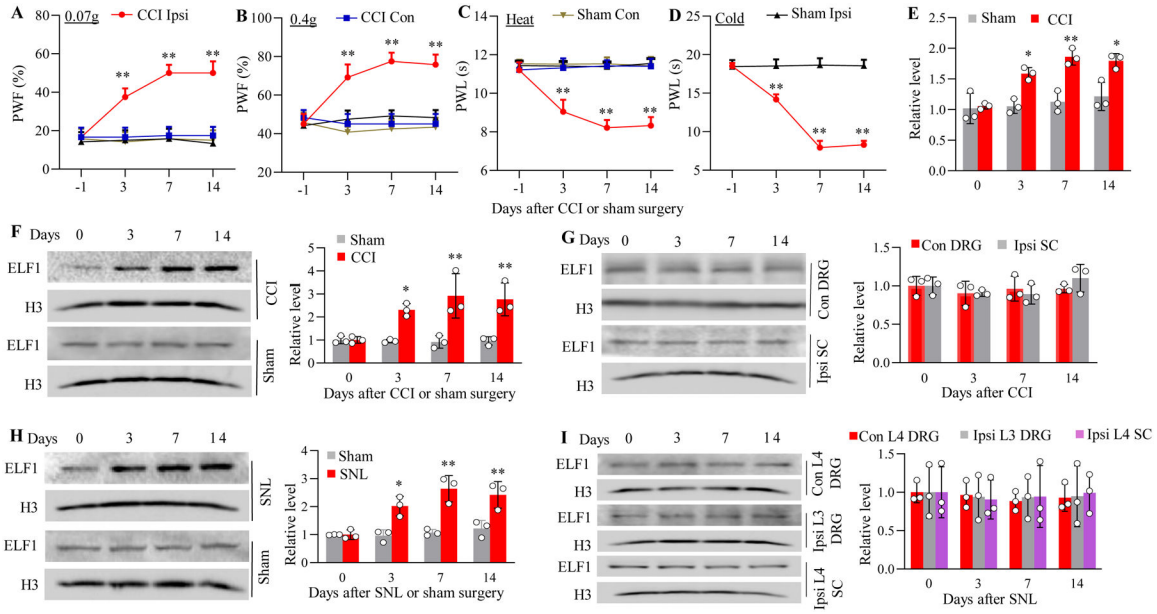

Fig. 1.

Peripheral nerve trauma-induced upregulation of ELF1 expression in injured DRG. (A-D) Paw withdrawal frequencies (PWF) to 0.07 g (A) and 0.4 g (B) von Frey filament stimuli and paw withdrawal latencies (PWL) to heat (C) and cold (D) stimuli on the ipsilateral (Ipsi) and contralateral (Con) on days −1, 3, 7 and 14 after CCI or sham surgery. n = 12 mice/group. Three-way ANOVA with repeated measures followed by post hoc Tukey test (Table S1). $^{**}P < 0.01$ *vs* sham group on the ipsilateral side at the corresponding time points. (E, F) Expression of *Elf1* mRNA (E) and ELF1 protein (F) in the ipsilateral L3/4 DRGs on days 0, 3, 7 and 14 after CCI or sham surgery. n = 3 experimental repeats (6 mice)/group. Two-way ANOVA followed by post hoc Tukey test (Table S1). $^{*}P < 0.05$, $^{**}P < 0.01$ *vs* sham group at the corresponding time points. (G) Expression of ELF1 protein in the contralateral (Con) L3/4 DRG and ipsilateral (Ipsi) L3/4 spinal cord dorsal horn (SC) on days 0, 3, 7 and 14 post-CCI. n = 3 experimental repeats (6 mice)/group. One-way ANOVA followed by post hoc Tukey test (Table S1). (H) Expression of ELF1 protein in the ipsilateral L4 DRG on days 0, 3, 7 and 14 after SNL or sham surgery. n = 3 experimental repeats (12 mice)/group. Two-way ANOVA followed by post hoc Tukey test (Table S1). $^{*}P < 0.05$, $^{**}P < 0.01$ *vs* sham group at the corresponding time points. (I) Expression of ELF1 protein in the contralateral (Con) L4 DRG, ipsilateral (Ipsi) L3 DRG and ipsilateral L4 spinal cord dorsal horn (SC) on days 0, 3, 7 and 14 after SNL. n = 3 experimental repeats (12 mice)/group. One-way ANOVA followed by post hoc Tukey test (Table S1).

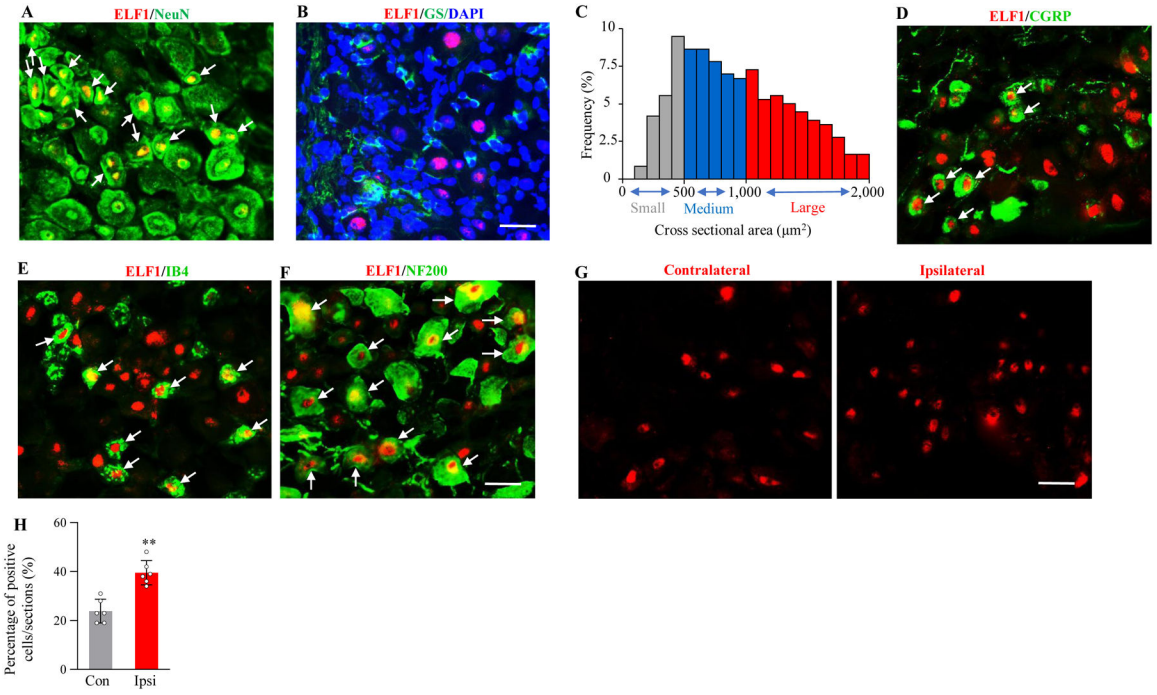

Fig. 2.

Distribution of ELF1 protein in lumbar DRG of naïve and CCI mice. (A, B) Double-labelled immunofluorescent assay showed co-localization (arrows) of ELF1 (red) with NeuN (green; A), but not with glutamine synthetase (GS; green; B), in the DRG cells. B: Cellular nuclei were labelled by 4',6-diamidino-2-phenylindole (DAPI; blue). n = 3 mice. Scale bar, 50 μm. (C) Size distribution of ELF1-positive neuronal somata in naïve DRG. small: 20.1%; Large, medium: 38.7%; 41.2%. (D-F) Double-labelled immunofluorescent staining (arrows) of ELF1 (red) with calcitonin gene-related peptide (CGPR; green, d), isolectin B4 (IB4; green, e) or neurofilament 200 (NF200; green, f) in DRG neurons. n = 3 mice. Scale bar, 50 μm. (G, H) Neurons labelled by ELF1 in the contralateral (Con) and ipsilateral (Ipsi) L4 DRG on day 7 post-CCI. G: Representative immunostaining images. H: Statistical summary of the number of ELF1-labeled neurons. n = 3 mice. $^{**}P < 0.01$ *vs* the contralateral side by two-tailed unpaired Student's *t*-test. Scale bar: 50 μm.

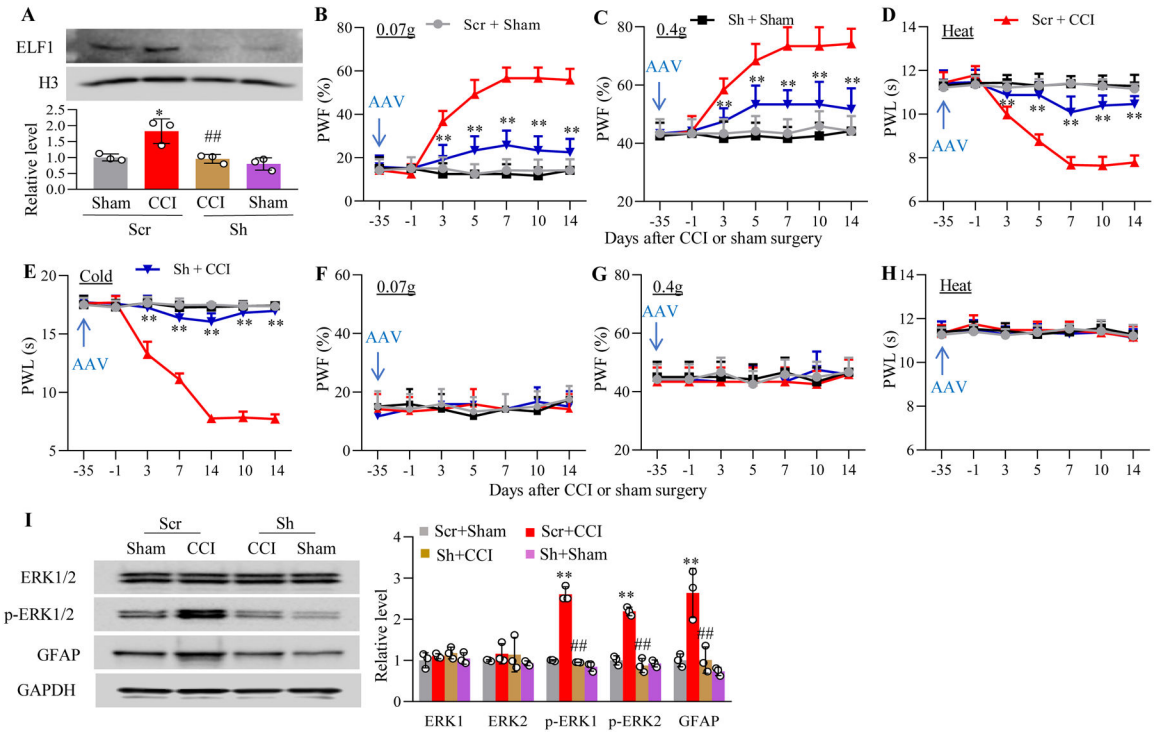

Fig 3.

Effect of DRG microinjection of AAV5-*Elf1* shRNA on CCI-induced nociceptive hypersensitivities and dorsal horn central sensitization during the development period in male mice. (A) Expression of ELF1 protein in the ipsilateral L3/4 DRGs on day 14 after CCI or sham surgery in mice microinjected with AAV5-*Elf1* shRNA (Sh) or negative control AAV5-scramble shRNA (Scr). n = 3 experimental repeats (6 mice) /group. Two-way ANOVA followed by post hoc Tukey test (Table S1). $*P < 0.05$ *vs* the scrambled shRNA plus sham group. $\#\#P < 0.01$ *vs* the scrambled shRNA plus CCI group. (B-H) Effect of microinjection of AAV5-*Elf1* shRNA (Sh) or negative control AAV5-scrambled shRNA (Scr) into the ipsilateral L3/L4 DRGs on paw withdrawal frequencies (PWF) to 0.07 g (B, F) and 0.4 g (C, G) von Frey filament stimuli and paw withdrawal latency (PWL) to heat (D, H) and cold (E) stimuli on the ipsilateral (B-E) and contralateral (F-H) sides at the different days as indicated after CCI or sham surgery. n = 12 mice/group. Three-way ANOVA with repeated measures followed by post hoc Tukey test (Table S1). $**P < 0.01$ *vs* the scrambled shRNA plus CCI group at the corresponding time points. (I) Effect of microinjection of AAV5-*Elf1* shRNA (Sh) or negative control AAV5-scrambled shRNA (Scr) into the ipsilateral L3/L4 DRGS on the expression of p-ERK1/2, total ERK1/2 and GFAP in the ipsilateral L3/L4 dorsal horn on day 14 after CCI or sham surgery. Left: representative Western immunoblots. Right: statistical summary of densitometric analysis. n = 3 mice/group. Two-way ANOVA followed by post hoc Tukey test (Table S1). $**P < 0.01$ *vs* the corresponding scrambled shRNA plus sham group. $\#\#P < 0.01$ *vs* the corresponding scrambled shRNA plus CCI group.

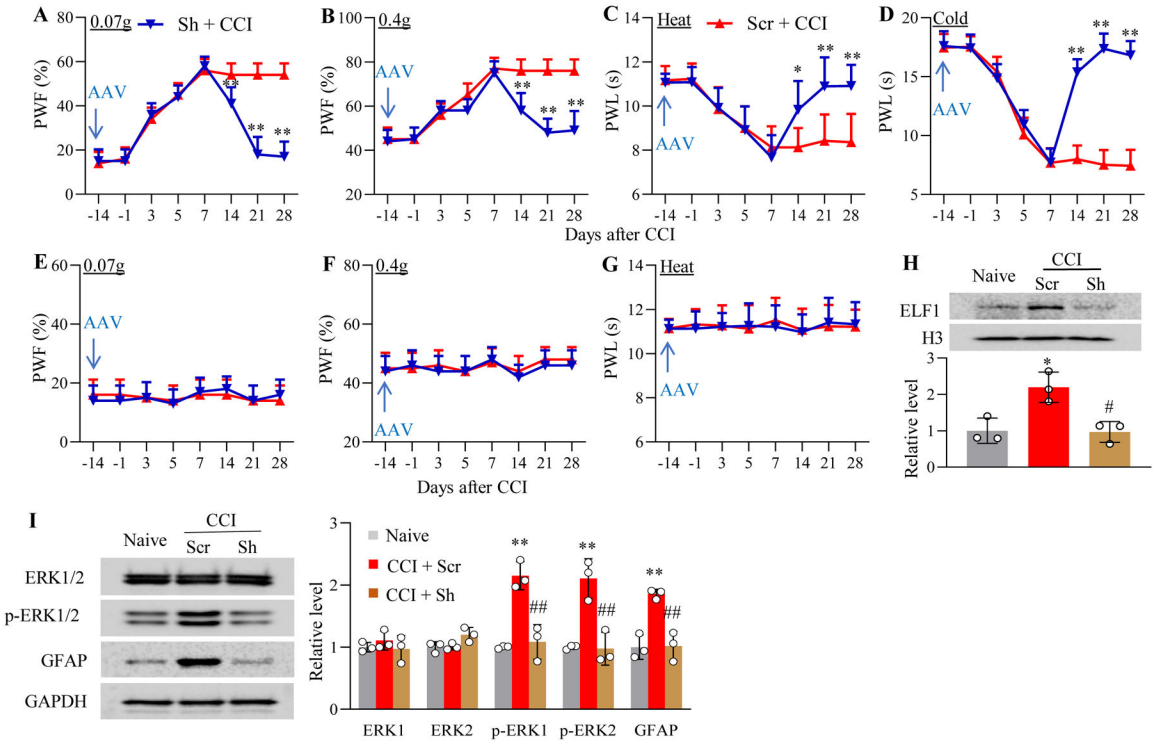

Fig 4.

Effect of DRG microinjection of AAV5-*Elf1* shRNA on CCI-induced nociceptive hypersensitivities and dorsal horn central sensitization during the maintenance period. (A-G) Effect of microinjection of AAV5-*Elf1* shRNA (Sh) or negative control AAV5-scrambled shRNA (Scr) into the ipsilateral L3/4 DRGs 14 days before CCI on paw withdrawal frequencies (PWF) to 0.07 g (A, E) and 0.4 g (B, F) von Frey filament stimuli and paw withdrawal latency (PWL) to heat (C, G) and cold (D) stimuli on the ipsilateral (A-D) and contralateral (E-G) sides at the different days as indicated after CCI surgery. n = 10 mice/group. Two-way ANOVA with repeated measures followed by post hoc Tukey test (Table S1). $*P < 0.05$, $**P < 0.01$ *vs* the scrambled shRNA plus CCI group at the corresponding time points. (H) Expression of ELF1 protein in the ipsilateral L3/4 DRGs on day 28 post-CCI in mice microinjected with AAV5-*Elf1* shRNA (Sh) or control AAV5-scrambled shRNA (Scr). L3/4 DRGs from naive mice were used as the control. n = 3 experimental repeats (6 mice)/group. One-way ANOVA followed by post hoc Tukey test (Table S1). $*P < 0.05$ *vs* the scramble shRNA plus CCI group on the contralateral side. $\#P < 0.05$ *vs* the scrambled shRNA plus CCI group on the ipsilateral side. (I) Effect of microinjection of AAV5-*Elf1* shRNA (Sh) or negative control AAV5-scrambled shRNA (Scr) into the ipsilateral L3/4 DRGs on expression of p-ERK1/2, total ERK1/2 and GFAP in the ipsilateral L3/4 dorsal horn on day 28 after CCI. L3/4 DRGs from naive mice were used as the control. Left: representative Western immunoblots. Right: statistical summary of densitometric analysis. n = 3 mice/group. One-way ANOVA followed by post hoc Tukey test (Table S1). $**P < 0.01$ *vs* the corresponding scrambled shRNA plus CCI group on the contralateral side. $\#\#P < 0.01$ *vs* the corresponding scrambled shRNA plus CCI group on the ipsilateral side.

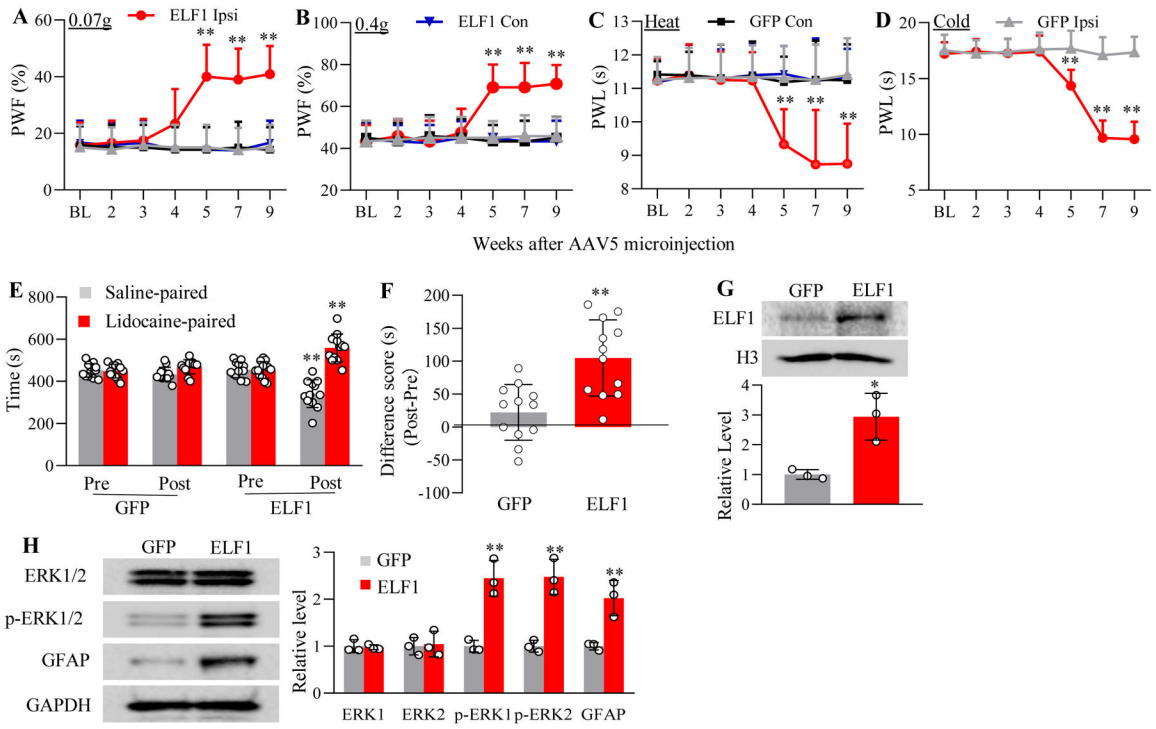

Fig 5.

Effect of DRG ELF1 overexpression on nociceptive thresholds and dorsal horn central sensitization in naïve male mice. (A-D) Effect of microinjection of AAV5-*Elf1* (Elf1) or AAV5-*Gfp* (GFP) into the unilateral L3/4 DRGs on paw withdrawal frequencies (PWF) to 0.07 g (A) and 0.4 g (B) von Frey filament stimuli and paw withdrawal latency (PWL) to heat (C) and cold stimuli (D) on the ipsilateral (Ipsi) and contralateral (Con) sides at the different weeks as indicated post-viral microinjection. BL, baseline. n = 12 mice/group. Three-way ANOVA (A-C; Table S1) or two-way ANOVA (D; Table S1) with repeated measures followed by post hoc Tukey test. $^{**}P < 0.01$ *vs* the AAV5-*Gfp* group on the ipsilateral side at the corresponding time points. (E, F) Effect of microinjection of AAV5-*Elf1* or AAV5-*Gfp* into the unilateral L3/4 DRGs on spontaneous ongoing pain as assessed by the CPP paradigm. E: Time spent in each chamber. F: Difference scores for chamber preference were calculated by subtracting preconditioning preference time from postconditioning time spent in the lidocaine-paired chamber. Post, post-conditioning. Pre, preconditioning. n = 12 mice/group. $^{**}P < 0.01$ *vs* the corresponding preconditioning by three-way ANOVA followed by Tukey post hoc test (E; Table S1) or *vs* the AAV5-*Gfp* group by two-tailed unpaired Student's *t* test (F; Table S1). (G) Level of ELF1 protein in the ipsilateral L3/4 DRGs 9 weeks after microinjection of AAV5-*Elf1* (ELF1) or control AAV5-*Gfp* (GFP). n = 6 mice/group. $^{*}P < 0.05$ *vs* the AAV5-*Gfp* group by two-tailed unpaired Student's *t* test (Table S1). (H) Effect of microinjection of AAV5-*Elf1* (ELF1) or AAV5-*Gfp* (GFP) into the unilateral L3/4 DRGs on the amounts of p-ERK1/2, total ERK1/2 and GFAP in the ipsilateral L3/4 dorsal horn 9 weeks after viral microinjection. Representative Western immunoblots (left) and a summary of the densitometric analysis (right) are shown. n = 3 mice/group. $^{**}P < 0.01$ *vs* the corresponding AAV5-*Gfp* group by two-tailed unpaired Student's *t* test (Table S1).

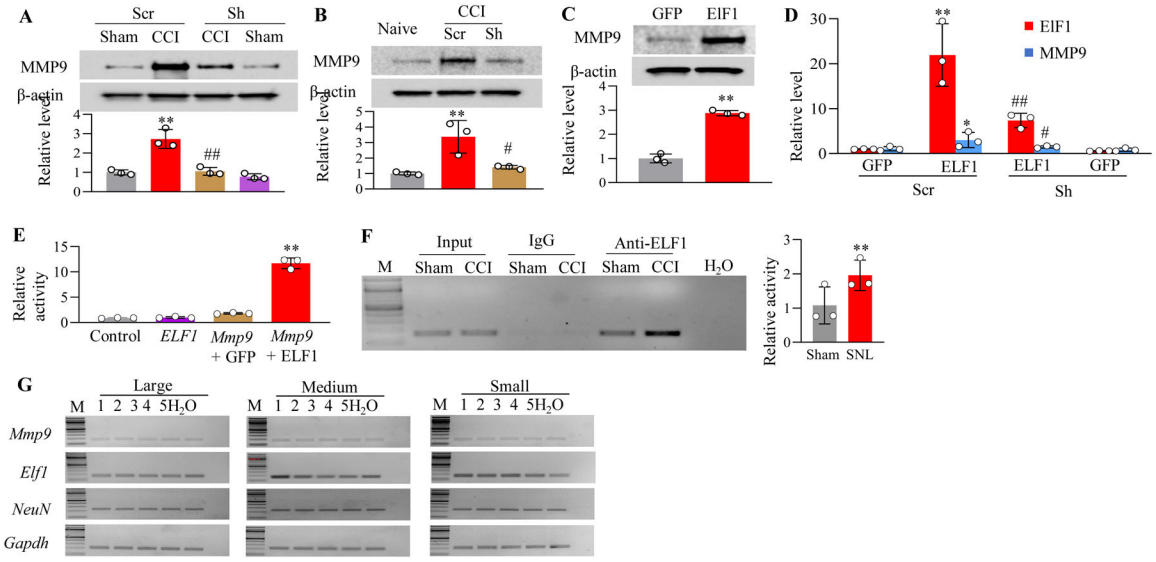

Fig 6.

Role of increased DRG ELF1 in CCI-induced upregulation of MMP9 in injured DRG. (A) Expression of MMP9 in the ipsilateral L3/4 DRGs on day 14 after CCI or sham surgery in mice microinjected with AAV5-*Elf1* shRNA (Sh) or negative control AAV5-scrambled shRNA (Scr). Representative Western immunoblots (upper) and a statistical summary of the densitometric analysis (bottom) are shown. n = 3 experimental repeats (6 mice)/group. Two-way ANOVA followed by post hoc Tukey test (Table S1). $^{**}P < 0.01$ vs the scrambled shRNA plus sham group. $^{\#\#}P < 0.01$ *vs* the scrambled shRNA plus CCI group. (B) Expression of MMP9 protein in the ipsilateral L3/4 DRGs on day 28 after CCI in mice microinjected with AAV5- *Elf1* shRNA (Sh) or negative control AAV5-scrambled shRNA (Scr). L3/4 DRGs from naive mice were used as the control. n = 3 experimental repeats (6 mice)/group. One-way ANOVA followed by post hoc Tukey test (Table S1). $^{**}P < 0.01$ *vs* the scrambled shRNA plus CCI group on the contralateral side. $^{\#}P < 0.05$ *vs* the scrambled shRNA plus CCI group on the ipsilateral side. (C) Expression of MMP9 protein in the ipsilateral L3/4 DRGs 9 weeks after microinjection of AAV5-*Elf1* (ELF1) or control AAV5-*Gfp* (GFP) in naïve mice. Representative Western immunoblots (upper) and a statistical summary of the densitometric analysis (bottom) are shown. n = 3 experimental repeats (6 mice)/group. $^{**}P < 0.01$ *vs* the AAV5-*Gfp* group by two-tailed unpaired Student's *t* test (Table S1). (D) Expression of *Elf1* mRNA in mouse cultured DRG neurons transduced as indicated. GFP: AAV5-*Gfp*. ELF1: AAV5-*Elf1*. Scr: control negative AAV5-scrambled shRNA. Sh: AAV5-*shElf1*. n = 3 experimental repeats/group. One-way ANOVA followed by Tukey post hoc test (Table S1). $^{*}P < 0.05$, $^{**}P < 0.01$ *vs* the corresponding AAV5-*Gfp* plus AAV5-scrambled shRNA group. $^{\#}P < 0.05$, $^{\#\#}P < 0.01$ *vs* the corresponding AAV5-*Elf1* plus AAV5-scrambled shRNA group. (E) *Mmp9* gene promoter activity in CAD cells transfected with the vectors and transduced with virus as shown. Control: empty pGL3-Basic. *Mmp9*: pGL3-*Mmp9* vector. GFP: AAV5-*Gfp*. ELF1: AAV5-*Elf1*. n = 3 experimental repeats/group. One-way ANOVA followed by Tukey post hoc test (Table S1). $^{**}P < 0.01$ *vs* the AAV5-*Gfp* plus pGL3-*Mmp9* vector group. (F) The *Mmp9* promoter fragment immunoprecipitated by anti-ELF1 antibody in the ipsilateral L3/4

DRGs on day 7 post-CCI or sham surgery. Input: total purified fragments. M: ladder marker. n = 3 experimental repeats (15 mice)/group. $^{**}P < 0.01$ *vs* sham group by two-tailed paired Student's *t* test (Table S1). (g) Co-expression analysis of *Elf1* mRNA and *Mmp9* mRNA in individual large (> 35 μm in diameter), medium (25–35 μm in diameter) and small (< 25 μm in diameter) DRG neurons of naïve mice. *NeuN* mRNA is used as a marker for DRG neurons. *Gapdh* mRNA is used as a loading control. Number 1–5: five different neurons. M: DNA ladder marker. H_2O: no cDNA. n = 5 neurons/size.

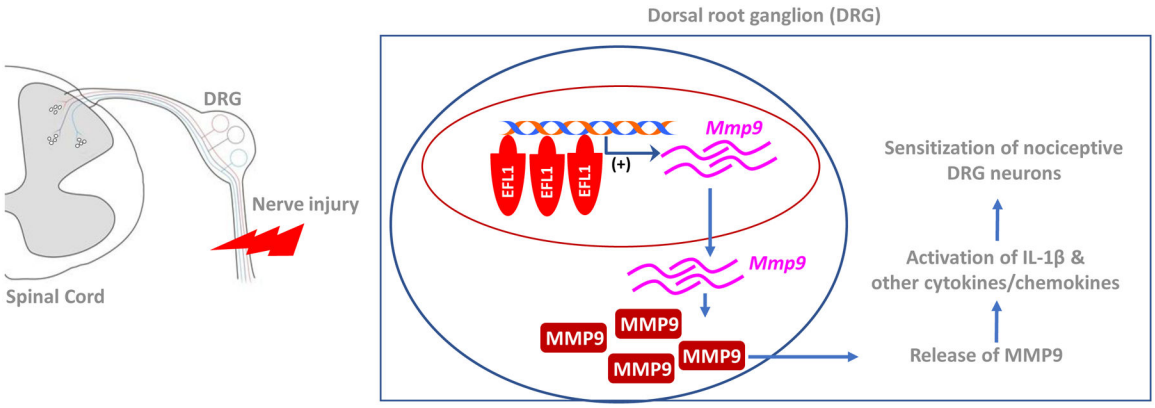

Fig. 7.

Schematic showing the mechanism by which ELF1 triggers MMP9 expression in injured DRG neurons after peripheral nerve trauma. Peripheral nerve trauma-induced upregulation of ELF1 triggers the transcriptional activation of *Mmp9* gene and then increases the levels of *Mmp9* mRNA and MMP9 proteins in injured DRG neurons. The released MMP9 activates IL-1β and other cytokines/chemokines through cleavage, resulting in the sensitization of nociceptive DRG neurons, consequently enhancing the release of neurotransmitters/neuromodulators in primary afferents and then leading to central sensitization in spinal cord dorsal horn.

Table 1:

Locomotor function.

Treatment groups	Placing	Grasping	Righting
Scr + Sham (male)	5 (0)	5 (0)	5 (0)
Scr + CCI (male)	5 (0)	5 (0)	5 (0)
Sh + CCI (male)	5 (0)	5 (0)	5 (0)
Sh + Sham (male)	5 (0)	5 (0)	5 (0)
Scr + Sham (female)	5 (0)	5 (0)	5 (0)
Scr + CCI (female)	5 (0)	5 (0)	5 (0)
Sh + CCI (female)	5 (0)	5 (0)	5 (0)
Sh + Sham (female)	5 (0)	5 (0)	5 (0)
GFP (male)	5 (0)	5 (0)	5 (0)
ELF1 (male)	5 (0)	5 (0)	5 (0)
GFP (female)	5 (0)	5 (0)	5 (0)
ELF1 (female)	5 (0)	5 (0)	5 (0)

n = 6–12 mice per group; 5 trials; Mean (SD). CCI: chronic constriction injury. GFP: green fluorescent protein. ELF1: E74-like factor 1. Scr: AAV5-scrambled shRNA. Sh: *AAV5-Elf1* shRNA.